

# The airborne lifetime of small speech droplets and their potential importance in SARS-CoV-2 transmission

Valentyn Stadnytskyi<sup>a</sup> , Christina E. Bax<sup>b</sup> , Adriaan Bax<sup>a,1</sup> , and Philip Anfinrud<sup>a,1</sup>

<sup>a</sup>Laboratory of Chemical Physics, National Institute of Diabetes and Digestive and Kidney Diseases, National Institutes of Health, Bethesda, MD 20892-0520; and <sup>b</sup>Perelman School of Medicine, University of Pennsylvania, Philadelphia, PA 19104

Edited by Axel T. Brunger, Stanford University, Stanford, CA, and approved May 4, 2020 (received for review April 10, 2020)

**Speech droplets generated by asymptomatic carriers of severe acute respiratory syndrome coronavirus 2 (SARS-CoV-2) are increasingly considered to be a likely mode of disease transmission. Highly sensitive laser light scattering observations have revealed that loud speech can emit thousands of oral fluid droplets per second. In a closed, stagnant air environment, they disappear from the window of view with time constants in the range of 8 to 14 min, which corresponds to droplet nuclei of ca. 4  $\mu\text{m}$  diameter, or 12- to 21- $\mu\text{m}$  droplets prior to dehydration. These observations confirm that there is a substantial probability that normal speaking causes airborne virus transmission in confined environments.**

COVID-19 | speech droplet | independent action hypothesis | respiratory disease | disease transmission

It has long been recognized that respiratory viruses can be transmitted via droplets that are generated by coughing or sneezing. It is less widely known that normal speaking also produces thousands of oral fluid droplets with a broad size distribution (ca. 1  $\mu\text{m}$  to 500  $\mu\text{m}$ ) (1, 2). Droplets can harbor a variety of respiratory pathogens, including measles (3) and influenza virus (4) as well as *Mycobacterium tuberculosis* (5). High viral loads of severe acute respiratory syndrome coronavirus 2 (SARS-CoV-2) have been detected in oral fluids of coronavirus disease 2019 (COVID-19)-positive patients (6), including asymptomatic ones (7). However, the possible role of small speech droplet nuclei with diameters of less than 30  $\mu\text{m}$ , which potentially could remain airborne for extended periods of time (1, 2, 8, 9), has not been widely appreciated.

In a recent report (10), we used an intense sheet of laser light to visualize bursts of speech droplets produced during repeated spoken phrases. This method revealed average droplet emission rates of ca. 1,000  $\text{s}^{-1}$  with peak emission rates as high as 10,000  $\text{s}^{-1}$ , with a total integrated volume far higher than in previous reports (1, 2, 8, 9). The high sensitivity of the light scattering method in observing medium-sized (10  $\mu\text{m}$  to 100  $\mu\text{m}$ ) droplets, a fraction of which remain airborne for at least 30 s, likely accounts for the large increase in the number of observed droplets. Here, we derive quantitative estimates for both the number and size of the droplets that remain airborne. Larger droplets, which are also abundant but associated with close-proximity direct virus transfer or fomite transmission (11), or which can become resuspended in air at a later point in time (12), are not considered here.

According to Stokes' law, the terminal velocity of a falling droplet scales as the square of its diameter. Once airborne, speech-generated droplets rapidly dehydrate due to evaporation, thereby decreasing in size (13) and slowing their fall. The probability that a droplet contains one or more virions scales with its initial hydrated volume, that is, as the cube of its diameter,  $d$ . Therefore, the probability that speech droplets pass on an infection when emitted by a virus carrier must take into account how long droplet nuclei remain airborne (proportional to  $d^{-2}$ ) and the probability that droplets encapsulate at least one virion (proportional to  $d^3$ ), the product of which is proportional to  $d$ .

The amount by which a droplet shrinks upon dehydration depends on the fraction of nonvolatile matter in the oral fluid, which includes electrolytes, sugars, enzymes, DNA, and remnants of dehydrated epithelial and white blood cells. Whereas pure saliva contains 99.5% water when exiting the salivary glands, the weight fraction of nonvolatile matter in oral fluid falls in the 1 to 5% range. Presumably, this wide range results from differential degrees of dehydration of the oral cavity during normal breathing and speaking and from decreased salivary gland activity with age. Given a nonvolatile weight fraction in the 1 to 5% range and an assumed density of 1.3  $\text{g}\cdot\text{mL}^{-1}$  for that fraction, dehydration causes the diameter of an emitted droplet to shrink to about 20 to 34% of its original size, thereby slowing down the speed at which it falls (1, 13). For example, if a droplet with an initial diameter of 50  $\mu\text{m}$  shrinks to 10  $\mu\text{m}$ , the speed at which it falls decreases from 6.8  $\text{cm}\cdot\text{s}^{-1}$  to about 0.35  $\text{cm}\cdot\text{s}^{-1}$ . The distance over which droplets travel laterally from the speaker's mouth during their downward trajectory is dominated by the total volume and flow velocity of exhaled air (8). The flow velocity varies with phonation (14), while the total volume and droplet count increase with loudness (9). Therefore, in an environment of stagnant air, droplet nuclei generated by speaking will persist as a slowly descending cloud emanating from the speaker's mouth, with the rate of descent determined by the diameter of the dehydrated speech droplet nuclei.

The independent action hypothesis (IAH) states that each virion has an equal, nonzero probability of causing an infection. Validity of IAH was demonstrated for infection of insect larvae by baculovirus (15), and of plants by Tobacco etch virus variants that carried green fluorescent protein markers (16). IAH applies to systems where the host is highly susceptible, but the extent to which IAH is valid for humans and SARS-CoV-2 has not yet been firmly established. For COVID-19, with an oral fluid average virus RNA load of  $7 \times 10^6$  copies per milliliter (maximum of  $2.35 \times 10^9$  copies per milliliter) (7), the probability that a 50- $\mu\text{m}$ -diameter droplet, prior to dehydration, contains at least one virion is  $\sim 37\%$ . For a 10- $\mu\text{m}$  droplet, this probability drops to 0.37%, and the probability that it contains more than one virion, if generated from a homogeneous distribution of oral fluid, is negligible. Therefore, airborne droplets pose a significant risk only if IAH applies to human virus transmission. Considering that frequent person-to-person transmission has been reported in community and health care settings, it appears likely that IAH

Author contributions: C.E.B., A.B., and P.A. designed research; V.S., A.B., and P.A. performed research; V.S. analyzed data; and C.E.B., A.B., and P.A. wrote the paper.

The authors declare no competing interest.

This open access article is distributed under [Creative Commons Attribution License 4.0 \(CC BY\)](https://creativecommons.org/licenses/by/4.0/).

Data deposition: Movies that show the experimental setup and the full 85-minute observation of speech droplet nuclei have been deposited at Zenodo and can be accessed at <https://doi.org/10.5281/zenodo.3770559>.

<sup>1</sup>To whom correspondence may be addressed. Email: bax@nih.gov or philip.anfinrud@nih.gov.

applies to COVID-19 and other highly contagious airborne respiratory diseases, such as influenza and measles.

## Results and Discussion

The output from a green (532 nm) Coherent Verdi laser operating at 4-W optical power was transformed with spherical and cylindrical optics into a light sheet that is  $\sim 1$  mm thick and 150 mm tall. This light sheet passed through slits centered on opposite sides of a cubic 226-L enclosure. When activated, a 40-mm, 12-V muffin fan inside the enclosure spatially homogenizes the distribution of particles in the enclosure. A movie showing the arrangement is available (17). Movie clips of speech droplet nuclei were recorded at a frame rate of 24 Hz with high-definition resolution ( $1,920 \times 1,080$  pixels). The camera lens provided a horizontal field of view of  $\sim 20$  cm. Therefore, the volume intercepted by the light sheet and viewed by the camera is  $\sim 30$  cm $^3$ . The total number of particles in the enclosure can be approximated by multiplying the average number of particles detected in a single movie frame by the volume ratio of the enclosure to the visualized sheet, which is  $\sim 7,300$ . Slow convection currents, at speeds of a few centimeters per second, remained for the duration of the recording. These convection currents are attributed to a 0.5 °C temperature gradient in the enclosure (bottom to top) that presumably is due to heat dissipated by the iPhone11 camera, which was attached to the front side of the enclosure. Since the net air flux across any horizontal plane of the enclosure is zero, this convection does not impact the average rate at which droplet nuclei fall to the bottom of the enclosure.

With the internal circulation fan turned on, the enclosure was purged with HEPA-filtered air for several minutes. Then, the purge shutter was closed, the movie clip was started, the speaker port was opened, and the enclosure was “filled” with speech droplets by someone repeating the phrase “stay healthy” for 25 s. This phrase was chosen because the “th” phonation in the word “healthy” was found to be an efficient generator of oral fluid speech droplets. The internal fan was turned off 10 s after speech was terminated, and the camera continued recording for 80 min. The movie clip was analyzed frame by frame to determine the number of spots/streaks whose maximum single-pixel intensity exceeded a threshold value of 30. Fig. 1 charts the time-dependent decrease in the number of scattering particles detected. We are not yet able to quantitatively link the observed

scattered light intensity to the size of the scattering particle because the light intensity varies across the sheet. However, the brightest 25% were found to decay more quickly than the dimmer fraction, with the two curves reasonably well described by exponential decay times of 8 and 14 min, respectively (Fig. 1A). These fits indicate that, near time 0, there were, on average, approximately nine droplet nuclei in the 30-cm $^3$  observation window, with the larger and brighter nuclei (on average) falling to the bottom of the enclosure at faster speeds than the smaller and dimmer ones.

With the assumption that the contents of the box are homogenized by the muffin fan at time 0, the average number of droplets found in a single frame near time 0 corresponds to *ca.* 66,000 small droplets emitted into the 226-L enclosure, or *ca.* 2,600 small droplet nuclei per second of speaking. If the particle size distribution were a delta function and the particles were uniformly distributed in the enclosure, the particle count would be expected to remain constant until particles from the top of the enclosure descend to the top of the light sheet, after which the particle count would decay linearly to background level. The observation that the decay profiles are approximately exponential points to a substantial heterogeneity in particle sizes, even after binning them into two separate groups.

The weighted average decay rate ( $0.085 \text{ min}^{-1}$ ) of the bright and dim fractions of particles (Fig. 1A) translates into a half-life in the enclosure of *ca.* 8 min. Assuming this half-life corresponds to the time required for a particle to fall 30 cm (half the height of the box), its terminal velocity is only  $0.06 \text{ cm s}^{-1}$ , which corresponds to a droplet nucleus diameter of  $\sim 4 \mu\text{m}$ . At the relative humidity (27%) and temperature (23 °C) of our experiment, we expect the droplets to dehydrate within a few seconds. A dehydrated particle of  $4 \mu\text{m}$  corresponds to a hydrated droplet of *ca.* 12- to 21- $\mu\text{m}$  diameter, or a total hydrated volume of  $\sim 60 \text{ nL}$  to  $320 \text{ nL}$  for 25 s of loud speaking. At an average viral load of  $7 \times 10^6$  per milliliter (7), we estimate that 1 min of loud speaking generates at least 1,000 virion-containing droplet nuclei that remain airborne for more than 8 min. These therefore could be inhaled by others and, according to IAH, trigger a new SARS-CoV-2 infection.

The longest decay constant observed by us corresponds to droplets with a hydrated diameter of  $\geq 12 \mu\text{m}$  when exiting the mouth. The existence of even smaller droplets has been

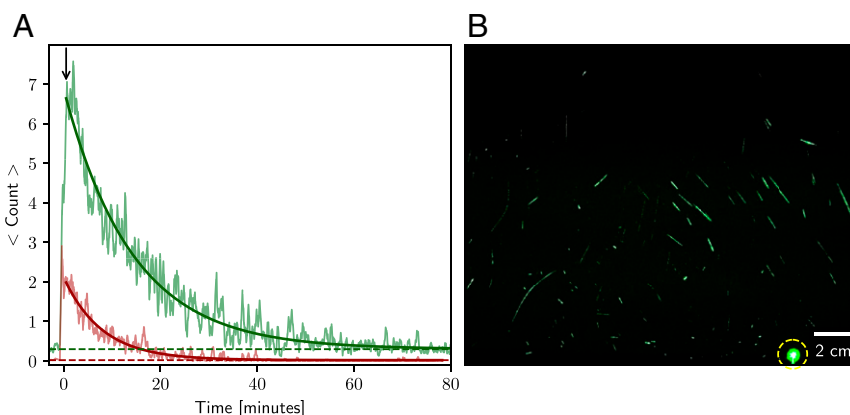


**Fig. 1.** Light scattering observation of airborne speech droplet nuclei, generated by a 25-s burst of repeatedly speaking the phrase “stay healthy” in a loud voice (maximum 85 dB<sub>B</sub> at a distance of 30 cm; average 59 dB<sub>B</sub>). (A) Chart of particle count per frame versus time (smoothed with a 24-s moving average), with the red curve representing the top 25% in scattering brightness and the green curve representing the rest. The bright fraction (red) decays with a time constant of 8 min, and the dimmer fraction (green) decays with a time constant of 14 min. Both exponential decay curves return to their respective background level of *ca.* 0 (red horizontal dashed line) and 0.4 (green dashed line) counts per frame. Time “0” corresponds to the time the stirring fan was turned off. The 25-s burst of speaking started 36 s before time 0. The black arrow (at 0.5 min) marks the start of the exponential fits. (B) Image of the sum of 144 consecutive frames (spanning 6 s) extracted shortly after the end of the 25-s burst of speaking. The dashed circle marks the needle tip used for focusing the camera. The full movie recording is available in ref. 17, with time “0” in the graph at time point 3:38 in the movie.

established by aerodynamic particle sizer (APS) measurements (2). APS is widely used for detecting aerosol particulates and is best suited for particles in the 0.5- to 5- $\mu\text{m}$  range. Morawska et al. (2) detected as many as 330 particles per second in the 0.8- to 5.5- $\mu\text{m}$  range upon sustained “aah” vocalization. Considering the short travel time (0.7 s) between exiting the mouth and the APS detector, and the high relative humidity (59%) used in that study, droplet dehydration may have been incomplete. If it were 75% dehydrated at the detector, an observed 5.5- $\mu\text{m}$  particle would have started as an 8.7- $\mu\text{m}$  droplet when exiting the mouth, well outside the 12- to 21- $\mu\text{m}$  range observed above by light scattering. This result suggests that APS and light scattering measurements form a perfect complement. However, we also note that, even while the smallest droplet nuclei effectively remain airborne indefinitely and have half-lives that are dominated by the ventilation rate, at a saliva viral load of  $7 \times 10^6$  copies per milliliter, the probability that a 1- $\mu\text{m}$  droplet nucleus (scaled back to its originally hydrated 3- $\mu\text{m}$  size) contains a virion is only 0.01%.

Our current setup does not detect every small particle in each frame of the movie, and our reported values are therefore conservative lower limit estimates. We also note that the saliva viral

load shows large patient-to-patient variation. Some patients have viral titers that exceed the average titer of Wölfel et al. by more than two orders of magnitude (7, 18), thereby increasing the number of virions in the emitted droplets to well over 100,000 per minute of speaking. The droplet nuclei observed in our present study and previously by APS (2, 9) are sufficiently small to reach the lower respiratory tract, which is associated with an increased adverse disease outcome (19, 20).

Our laser light scattering method not only provides real-time visual evidence for speech droplet emission, but also assesses their airborne lifetime. This direct visualization demonstrates how normal speech generates airborne droplets that can remain suspended for tens of minutes or longer and are eminently capable of transmitting disease in confined spaces.

**Data Availability Statement.** All raw data used for analysis are available in ref. 17.

**ACKNOWLEDGMENTS.** We thank Bernhard Howder for technical support, Clemens Wendtner, William A. Eaton, Roland Netz, and Steven Chu for insightful comments. This work was supported by the Intramural Research Program of the National Institute of Diabetes and Digestive and Kidney Diseases.

1. J. P. Duguid, The size and the duration of air-carriage of respiratory droplets and droplet-nuclei. *J. Hyg. (Lond.)* **44**, 471–479 (1946).
2. L. Morawska et al., Size distribution and sites of origin of droplets expelled from the human respiratory tract during expiratory activities. *J. Aerosol Sci.* **40**, 256–269 (2009).
3. L. Liljeroos, J. T. Huiskonen, A. Ora, P. Susi, S. J. Butcher, Electron cryotomography of measles virus reveals how matrix protein coats the ribonucleocapsid within intact virions. *Proc. Natl. Acad. Sci. U.S.A.* **108**, 18085–18090 (2011).
4. J. Yan et al.; EMIT Consortium, Infectious virus in exhaled breath of symptomatic seasonal influenza cases from a college community. *Proc. Natl. Acad. Sci. U.S.A.* **115**, 1081–1086 (2018).
5. K. P. Fennelly et al., Variability of infectious aerosols produced during coughing by patients with pulmonary tuberculosis. *Am. J. Respir. Crit. Care Med.* **186**, 450–457 (2012).
6. J. F.-W. Chan et al., Improved molecular diagnosis of COVID-19 by the novel, highly sensitive and specific COVID-19-RdRp/HeL real-time reverse transcription-polymerase chain reaction assay validated in vitro and with clinical specimens. *J. Clin. Microbiol.* **58**, e00310-20 (2020).
7. R. Wölfel et al., Virological assessment of hospitalized patients with COVID-2019. *Nature*, 10.1038/s41586-020-2196-x (2020).
8. C. Y. H. Chao et al., Characterization of expiration air jets and droplet size distributions immediately at the mouth opening. *J. Aerosol Sci.* **40**, 122–133 (2009).
9. S. Asadi et al., Aerosol emission and superemission during human speech increase with voice loudness. *Sci. Rep.* **9**, 2348 (2019).
10. P. Anfinrud, V. Stadnytskyi, C. E. Bax, A. Bax, Visualizing speech-generated oral fluid droplets with laser light scattering. *N. Engl. J. Med.*, 10.1056/NEJMcp2007800 (2020).
11. T. Raymond, Review of aerosol transmission of Influenza A virus. *Emerging Infect. Dis.* **J.** **12**, 1657–1662 (2006).
12. Y. Liu et al., Aerodynamic analysis of SARS-CoV-2 in two Wuhan hospitals. *Nature*, 10.1038/s41586-020-2271-3 (2020).
13. W. F. Wells, On air-borne infection—Study II droplets and droplet nuclei. *Am. J. Hyg.* **20**, 611–618 (1934).
14. H. Traunmüller, A. Eriksson, Acoustic effects of variation in vocal effort by men, women, and children. *J. Acoust. Soc. Am.* **107**, 3438–3451 (2000).
15. M. P. Zwart et al., An experimental test of the independent action hypothesis in virus-insect pathosystems. *Proc. Biol. Sci.* **276**, 2233–2242 (2009).
16. M. P. Zwart, J. A. Daròs, S. F. Elena, One is enough: In vivo effective population size is dose-dependent for a plant RNA virus. *PLoS Pathog.* **7**, e1002122 (2011).
17. V. Stadnytskyi, P. Anfinrud, C. E. Bax, A. Bax, The airborne lifetime of small speech droplets and their potential importance to SARS-CoV-2 transmission. *Zenodo*. <https://doi.org/10.5281/zenodo.3770559>. Deposited 10 April 2020.
18. C. Rothe et al., Transmission of 2019-nCoV infection from an asymptomatic contact in Germany. *N. Engl. J. Med.* **382**, 970–971 (2020).
19. R. Tellier, Y. Li, B. J. Cowling, J. W. Tang, Recognition of aerosol transmission of infectious agents: A commentary. *BMC Infect. Dis.* **19**, 101 (2019).
20. R. J. Thomas, Particle size and pathogenicity in the respiratory tract. *Virulence* **4**, 847–858 (2013).